RESEARCH ON A SYSTEM NOISE SIMULATION AND FILTERING METHOD IN TUNABLE DIODE LASER ABSORPTION SPECTROSCOPY TECHNOLOGY**

Wang Yan [1], Wang Fang [2], Zhang Rui [2], Yan Bo [3*], Si-Yan Yang [2], Xin-Bo Li [2]

[1] School of Computer and Information Engineering at Tianjin Chengjian University, Tianjin, China
[2] College of Electronic Information and Automation at Tianjin University of Science & Technology, Tianjin, China
[3] College of Electrical Engineering at Hebei University of Architecture, Zhangjiakou, China; e-mail: zhangrui@tust.edu.cn

To solve the problem of multiple noise interference when tunable diode laser absorption spectroscopy (TDLAS) technology is used for gas concentration detection, the principles of Kalman, moving average, wavelet transform, and singular value decomposition four filtering algorithm principles and system noise sources are analyzed. MATLAB simulation software is used to simulate the relationship curve of thermal noise, shot noise, relative intensity noise of lasers, and the characteristic value of harmonic signals. Four filtering algorithms are used to process the noise, and the best filtering algorithm is selected. Moreover, a TDLAS experimental system with ethylene gas as the detection object is designed in this paper. The experimental results show that the singular value decomposition method among the four filtering algorithms has the best effect in removing thermal noise, shot noise and laser noise. After filtering is performed, the accuracy of the continuous detection of the system is improved, and the purpose of reducing or even eliminating system noise can be achieved. After processing occurs, the signal-to-noise ratio of the detected signal of the system is improved by 57 dB, and the noise removal rate of the system reaches 66.7%.

Keywords: *tunable diode laser absorption spectrum, filtering algorithm, noise simulation, ethylene.*

МОДЕЛИРОВАНИЕ ШУМА И МЕТОДЫ ЕГО ФИЛЬТРАЦИИ В ДИОДНО-ЛАЗЕРНОЙ АБСОРБЦИОННОЙ СПЕКТРОСКОПИИ

W. Yan [1], W. Fang [2], Z. Rui [2], Y. Bo [3*], S.-Y. Yang [2], X.-B. Li [2]

УДК 543.42;535.34

[1] Школа компьютерной и информационной инженерии Тяньцзиньского университета Чэнцзянь, Тяньцзинь, Китай
[2] Колледж электронной информации и автоматизации Тяньцзиньского университета науки и технологий, Тяньцзинь, Китай
[3] Колледж электротехники при Хэбэйском архитектурном университете, Чжанцзякоу, Китай; e-mail: zhangrui@tust.edu.cn

(Поступила 12 июля 2022)

Для решения проблемы многократных шумовых помех в технологии перестраиваемой диодно-лазерной спектроскопии поглощения (TDLAS) при обнаружении концентрации газа использованы принципы Калмана, скользящее среднее, вейвлет-преобразование и разложение по сингулярным числам. Проанализированы четыре алгоритма фильтрации и система шумоподавления. С помощью программы MATLAB смоделированы зависимости теплового шума, дробового шума, шума относительной интенсивности лазеров и характеристического значения гармонических сигналов. Для обработки шума использованы четыре алгоритма фильтрации, среди которых выбран наилучший. Для

** Full text is published in JAS V. 90, No. 4 (http://springer.com/journal/10812) and in electronic version of ZhPS V. 90, No. 4 (http://www.elibrary.ru/title_about.asp?id=7318; sales@elibrary.ru).

проверки работоспособности предложенных алгоритмов шумоподавления разработана экспериментальная система TDLAS с газообразным этиленом в качестве объекта детектирования. Показано, что из четырех алгоритмов фильтрации метод сингулярного разложения дает наилучший эффект при удалении теплового, дробового и лазерного шумов. После выполнения фильтрации точность непрерывного обнаружения системы повышается, может быть достигнуто снижение или даже устранение системного шума. После обработки отношение сигнал/шум обнаруженного сигнала системы улучшается на 57 дБ, коэффициент шумоподавления системы достигает 66.7%.

Ключевые слова: *спектр поглощения перестраиваемого диодного лазера, алгоритм фильтрации, имитация шума, этилен.*

Introduction. Tunable semiconductor laser absorption spectroscopy is a gas concentration measurement technology formed by combining two technologies of laser modulation and absorption spectroscopy [1–3]. This technology has the characteristics of a high spectral resolution, high sensitivity, strong practicability, easy upgrading and online noncontact detection. However, its system has various interference noises when detecting trace gases, which in turn leads to problems such as low measurement limits and poor stability [4–6]. To obtain a relatively pure spectral line absorption signal so that the calculation result is less affected by system factors, it is necessary to eliminate the noise of the detection signal. Regarding the effective removal of system noise, Ruxton et al. [7–9] used delay fibers to eliminate residual amplitude modulation (RAM) and used dual optical paths for background acquisition and elimination. Reid et al. [10–13] used additional modulation methods to eliminate the optical interference fringes caused by the etalon of the optical system. The preceding method can effectively suppress the residual amplitude modulation and optical interference fringes, but the requirements for the equipment are higher in the implementation process, which increases the complexity of the system. Thus, this method is difficult to implement. Werle et al. [14] performed spectral line subtraction on background signals during zero ventilation. With this method, background signals that are not related to volume fractions, such as nonlinearities, can be effectively eliminated. This method is suitable for situations in which the background gas composition is known and the content remains unchanged.

In recent years, the filtering of algorithms has been greatly developed. Commonly used filtering algorithms include the Kalman filtering method, S-G smoothing filtering method, wavelet transform filtering method, genetic algorithm, particle swarm algorithm, and so on. Zhou Xiaowei [15] and others applied the Kalman filter algorithm to TDLAS concentration inversion to eliminate the influence of measurement noise and model errors on the experimental results; Hu Bo [16] used the SG smoothing filter method to process complex signals and designed a TDLAS system that performs data integration; Zou Debao [17] and others analyzed the selection of digital filtering methods in TDLAS escape ammonia detection, indicating that the arithmetic mean-wavelet transform filtering method can more effectively improve the original spectral signal. However, from the perspective of simulation, the research on the algorithms for noise removal is not sufficient.

We research the noise cancellation method of TDLAS technology for gas concentration detection using four filtering algorithms to determine the best filtering algorithm. By comparing the noise removal effect of the second simulated harmonic signal with different parameters in each algorithm, a set of parameters with the best noise removal effect is selected for the algorithm. Then, the simulation results of the four algorithms are compared and show that the SVD algorithm has a good denoising effect. To show the denoising ability of the real data, a physical TDLAS experimental system with ethylene gas as the detection object was designed. On this system, we verified, evaluated, and compared the denoising ability of four filtering algorithms. In the end, the experimental results show that the SVD method has the best practical denoising ability, which further promotes the research of TDLAS technology in eliminating the noise of measurement data.

Methodology. TDLAS is a type of infrared absorption spectrum detection. It is based on the Lamber–Beer law and uses wavelength modulation technology to add sinusoidal current for modulation in the form of:

$$,I_t = I_0 \exp[-\alpha(\nu)CL], \quad (1)$$

where I_t is the emission light intensity after gas absorption, I_0 is the initial light intensity without gas absorption, $\alpha(\nu)$ is the absorption coefficient of frequency at frequency ν, C is the concentration of measured gas, and L is the length of the absorption medium, which is the optical path length of the gas absorption. The absorption coefficient can be expressed as:

$$\alpha(\nu) = S(T)g(\nu)P, \quad (2)$$

where $S(T)$ refers to the absorption line strength, which is the function expression under the temperature T; $g(\nu)$ refers to the line strength function expression, which represents the linear function of the gas absorption spectrum line; and P is the gas pressure. Therefore, in an ideal situation, when the external conditions are constant and the incident light intensity is fixed, the emitted light intensity can be detected by the photoelectric detector to reverse the performance of the gas concentration.

In TDLAS technology, system noise includes thermal noise, shot noise, flicker noise, residual amplitude modulation noise, laser noise, etc. Among the aforementioned noises, if the system uses a 30 kHz high-frequency modulation signal, the flicker noise is very small and can be ignored; the remaining amplitude modulation noise can be eliminated by the delay fiber; the laser noise has a certain random characteristic, which can be filtered out by subsequent data processing. Due to the random characteristics of thermal noise, shot noise and laser noise, random time series are used to replace three kinds of noise in the simulation. Four filtering algorithms, Kalman, moving average, wavelet transform and SVD, are used for filtering.

The signal-to-noise ratio (SNR) and smoothness (R) are used as the evaluation indices of the denoising result:

$$\mathrm{SNR} = 10\lg \frac{\sum_{k=1}^{K} |s(k)|^2}{\sum_{k=1}^{K} |y(k) - s(k)|^2}, \tag{3}$$

$$R = \frac{\sum_{k=0}^{K-1} [y(k+1) - y(k)]^2}{\sum_{k=0}^{K-1} [s(k+1) - s(k)]^2}, \tag{4}$$

where $y(k)$ is the denoised signal and $s(k)$ is the original signal without noise. Moreover, the larger the SNR of the denoised signal is, the better the denoising effect. R indicates the smoothness of the signal; that is, the smaller the value of the smoothness is, the better the denoising effect of the filtering algorithm used for the signal to be analyzed. Furthermore, the closer the value of R is to 1, the closer the fluctuation of the signal after denoising is to that of the original signal without noise. The two evaluation indicators, SNR and R, are comprehensively considered to compare the final denoising effect.

Simulation modeling. We use Simulink to simulate the TDLAS detection system and noise. The model includes a gas module, a noise module and a data detection module. The standard second harmonic ($2f$) signal obtained by simulation is shown in Fig. 1a. Due to the random characteristics of thermal noise, shot noise and laser noise, in the simulation, random time series are used here to replace the three kinds of noise. The signal after adding noise to the standard second harmonic signal is shown in Fig. 1b.

The Kalman, moving average, wavelet transform and singular value decomposition methods are used to filter out the noise signal added in the simulation signal. The filter analysis is as follows.

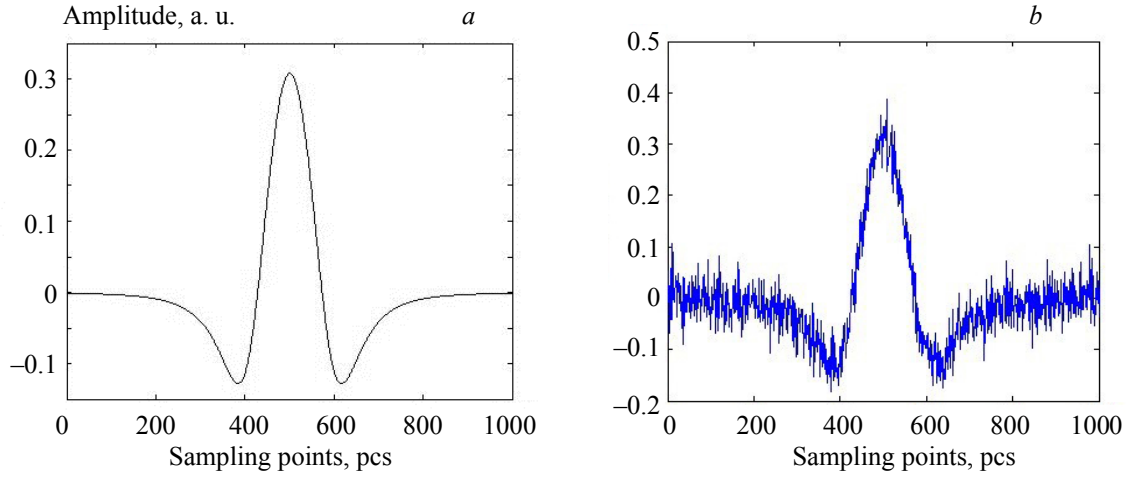

Fig. 1. Standard $2f$ signal (a) and with noise (b).

Use Kalman to filter out the noise signal added to the simulation signal. The Kalman filter is used to estimate the state variables of a discrete-time process, which is described by a discrete stochastic difference equation: $x_k = Ax_{k-1} + Bu_{k-1} + w_{k-1}$. Among them, the n-dimensional vector x_k is the system state variable at time k, and the n-dimensional vector x_{k-1} is the system state variable at time $k-1$. A is called the state transition matrix (or gain matrix), which is a square matrix of order n^*n. A connects the state at time k–1 with the state at time k in the past. The $n\times l$-order matrix B represents the gain of the optional control input $u\in R^l$. In many practical situations, there is no control gain, so this term is often 0 in practice; w_{k-1} is an n-dimensional vector representing process excitation noise, which corresponds to the noise of each component in x_k, and is Gaussian white noise with an expectation of 0 and a covariance of Q. In some stable processes, the Q value is determined, and the task at this time is to find the optimal Q value. To obtain the optimal Q value by adjusting the filter coefficients, we first specify a process excitation noise covariance matrix Q_0:

$$Q_0 = \begin{pmatrix} 1e-4 & 0 & 0 \\ 0 & 1e-4 & 0 \\ 0 & 0 & 1e-4 \end{pmatrix}. \quad (5)$$

The results are shown in Table 1 for when $0.1Q_0$, Q_0, $10Q_0$, $100Q_0$, and $1000Q_0$ are used as the process excitation noise covariance matrix for filtering, and the signal after Kalman filtering is shown in Fig. 2. The conclusion shows that when the state transition process is determined, the value of Q is best at approximately $100Q$. When the value of Q gradually increases, the filter convergence becomes slower, and the disturbance of the state variables becomes larger.

TABLE 1. Results of Kalman Filtered Processing

Filter parameter	SNR, dB	R
$0.1Q$	0.59	4.14
Q	3.5	1.59
$10Q$	10.28	0.56
$100Q$	15.63	0.12

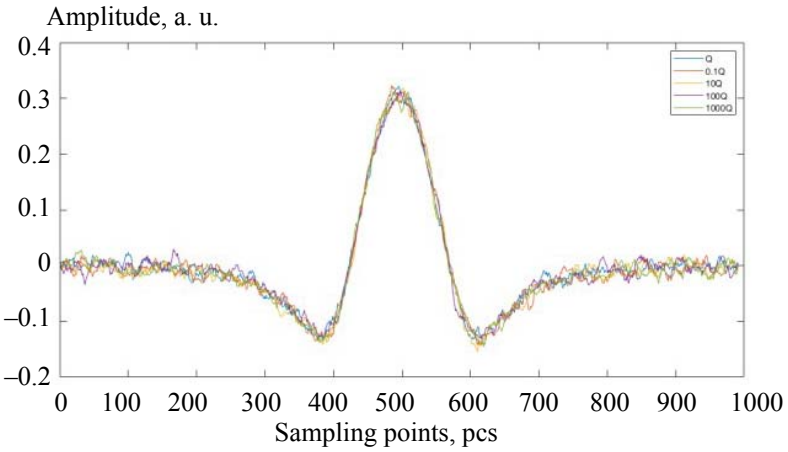

Fig. 2. 2*f* signal diagram after Kalman filtered processing at different parameters.

Use wavelet to filter out the noise signal added to the simulation signal. "Wavelets" are small waveforms. The term "small" refers to its attenuation, and the term "wave" refers to its volatility and its amplitude of positive and negative oscillations. Compared with the Fourier transform, the wavelet transform is a localized analysis of time (space) frequency. It gradually refines the signal (function) at multiple scales through expansion and translation operations and finally achieves time subdivision at high frequencies and frequency subdivision at low frequencies [18]. It can automatically adapt to the requirements of time-frequency signal analysis so that it can focus on any details of the signal and solve the difficult problem of the Fourier transform. The results of comparing the influence of different wavelet bases and threshold calculation methods on the denoising effect are shown in Table 2, and the signal after wavelet filtering is performed is shown in Fig. 3.

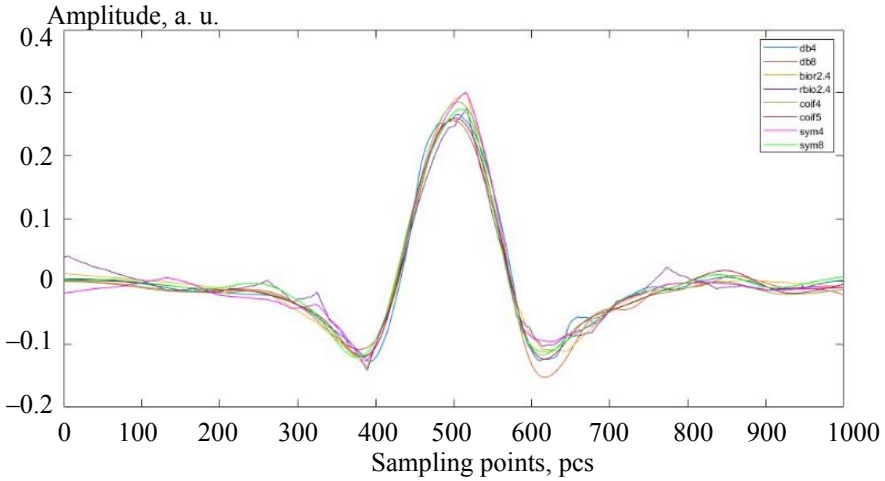

Fig. 3. 2*f* signal diagram after wavelet filtered processing at different parameters.

TABLE 2. Results of Wavelet filtered Processing

Wavelet basis function	Orthogonal filter bank	Length/point	Soft/hard threshold	SNR, dB	*R*
Daubechies	db4	8	soft	15.71	1.71
			hard	19.2	0.9
	db8	16	soft	14.78	1.26
			hard	18.4	0.53
Biorthonormal wavelet basis	bior2.4	10	soft	15.49	1.18
			hard	19.77	0.38
Anti-biortho-gonal wavelet	rbio2.4	10	soft	12.4	0.81
			hard	16.66	0.12
Coiflets	coif4	8	soft	16.32	1.17
			hard	20.38	1
	coif5	16	soft	14.89	1.19
			hard	18.07	0.95
Symlets	sym4	8	soft	15.01	1.19
			hard	19.12	1
	sym8	16	soft	16.52	1.06
			hard	19	0.9

The results show the following. The signal-to-noise ratio is higher after denoising the signal using the filter bank corresponding to the Coiflets wavelet base. The filter length has no effect on the denoising effect—for example, the filter length corresponding to db4 is half of the filter length corresponding to db8. When the soft threshold or hard threshold calculation method is used, the denoising effects of the two are very similar. In the processing method of wavelet coefficients, the hard threshold calculation method obtains a larger SNR and smaller smoothness than the soft threshold calculation method; thus, it is more suitable for noise removal. In general, choosing coif4 or a similar wavelet function for denoising and using a hard threshold calculation method can obtain better denoising results.

Use the moving average to filter out the noise signal added to the simulation signal. Moving average filtering is based on statistical law. It treats continuously sampled data as a queue with a fixed length of *N*. After a new measurement is obtained, the first data of the above queue are removed, the remaining *N*–1 data are moved forward in the sequence, and the newly sampled data are inserted as the tail of the new queue. Then, an arithmetic operation is performed on this queue, and the result is used as the result of this measurement. The effect of the sliding step length *L* on the denoising effect is shown in Table 3. The moving average filtered signal is shown in Fig. 4. The conclusion shows that when *L* is set to 24, the filtering effect is the best.

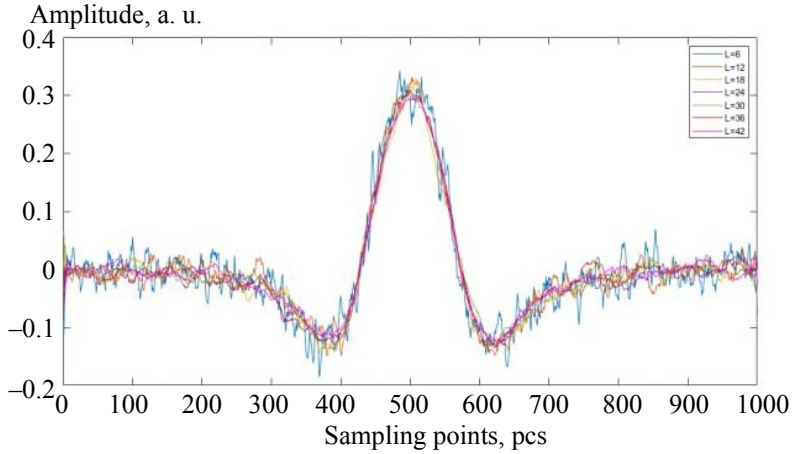

Fig. 4. 2*f* signal diagram after moving average filtered processing at different parameters.

TABLE 3. Results of Moving Average Filtered Processing

L	SNR, dB	*R*
6	15.76	0.16
12	19.82	0.47
18	20.14	0.65
24	23.82	0.8
30	19.1	0.94
36	19.82	0.68
42	17.32	1.78

Use SVD to filter out the noise signal added in the simulation signal. The singular value is a concept in the matrix, which is generally obtained by the singular value decomposition theorem. We let A be a matrix of order m^*n in the complex number domain, $q = \min(m,n)$, where m and n represent the number of rows and columns of the matrix, respectively. A^* denotes the conjugate transpose matrix of A, which can also be written as A^H. The arithmetic square root of the q nonnegative eigenvalues of A^*A is called the singular value of matrix A. Singular value decomposition is an important matrix decomposition method in linear algebra and matrix theory [19]. The effect of the number of singular values N on the denoising effect is shown in Table 4, and the signal after SVD filtering is shown in Fig. 5.

The conclusion shows that the SNR values under different N values are not much different, and when N is set to 8, the denoising effect is the best. The best value of the preceding four filtering algorithms is selected to filter out the noise signal added in the simulation signal again. Through comparison, the results show that the singular value decomposition method has the best filtering effect.

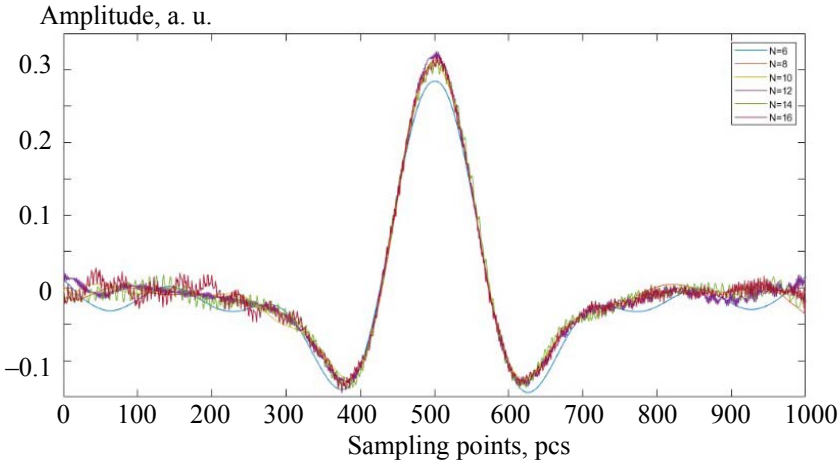

Fig. 5. 2*f* signal diagram after SVD filtered processing at different parameters.

TABLE 4. Results of SVD Filtered Processing

N	SNR, dB	*R*
6	9.39	1.069
8	10.17	1.228
10	10.22	0.508
12	10.76	0.422
14	10.86	0.334
16	11.08	0.093

Experimental. The experimental system consists of a standard gas module, TDLAS control board, laser, temperature control module, collimator, beam splitter, gas absorption cell, analog switch circuit module, detector, data acquisition card and host computer. The structure of the experimental system is shown in Fig. 6.

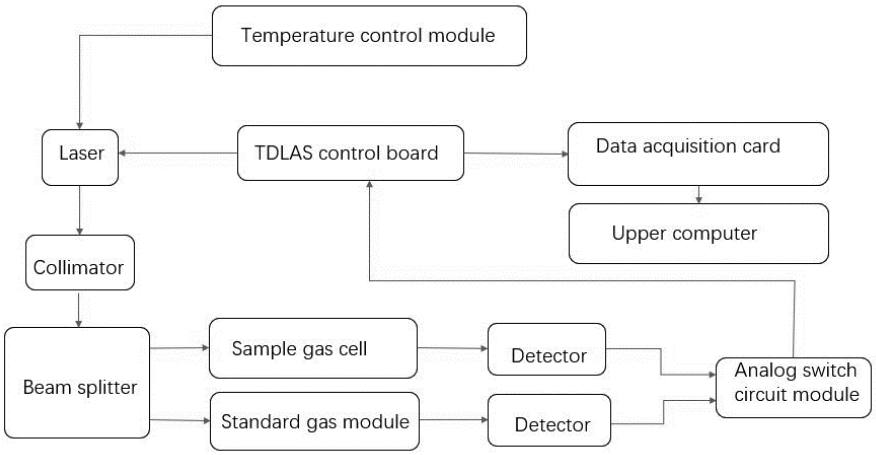

Fig. 6. Ethylene concentration detection system structure diagram.

Ethylene gas is selected as the detection object in the system. The standard gas module is a 50-ppm standard concentration ethylene gas module produced by Wavelength Electronics in the United States, and the TDLAS control board is PCI-FPGA-1A from Port City Instruments, LLC in the United States. The laser is a butterfly-packaged DFB pigtailed laser, with a center wavelength of 1626 nm, from Wuhan Oudi. The detector uses InGaAs with a working wavelength of 700–1800 nm photodiode. The temperature control board controls the working temperature of the DFB laser, and the sample gas cell has multiple reflection structures, increasing the optical path to 1 m. The data acquisition card adopts NI9222, produced by the NI company of the United States, and simultaneously collects the second harmonic signal and sawtooth wave scanning signal of gas.

Results and discussion. The working process of the detection system is as follows. The temperature control board roughly adjusts the laser temperature and positions the absorption frequency of the laser near the ethylene absorption spectrum line. The signal generating circuit on the TDLAS control board generates the low-frequency scanning signal and high-frequency modulation signal driving the laser wavelength change, and the two voltage signals are superposed and converted into the current signal to control the working current of the laser. The output wavelength of the laser is 1626 nm. After passing through the beam splitter, the laser enters the sample gas cell and the standard gas module and scans the absorption spectrum line of the measured gas. After passing through the sample gas cell and the standard gas module, the laser converts the optical signal into the electrical signal by the photodetector, and then the two electrical signals are transmitted to the TDLAS control board by the analog switch circuit module. Through the amplifier and the lock-in amplifier, the second harmonic signal is detected. The sawtooth frequency is 5 Hz, the peak value is 300 mV, the number of sampling points is 600, and the sampling period is 30. Finally, the data are collected by a data acquisition card and transmitted to a computer. Then, the data are processed with LabVIEW software. Lastly, the gas concentration detection results are obtained.

Figure 7a shows a section of the original second harmonic signal collected by this experimental system. There is a certain amount of noise in it, which will interfere with the 1626 nm absorption spectrum of ethylene and affect the detection accuracy. According to the simulation results, we set the optimal parameters corresponding to each algorithm to remove noise, and the processing effects are shown in Figs. 7b–e.

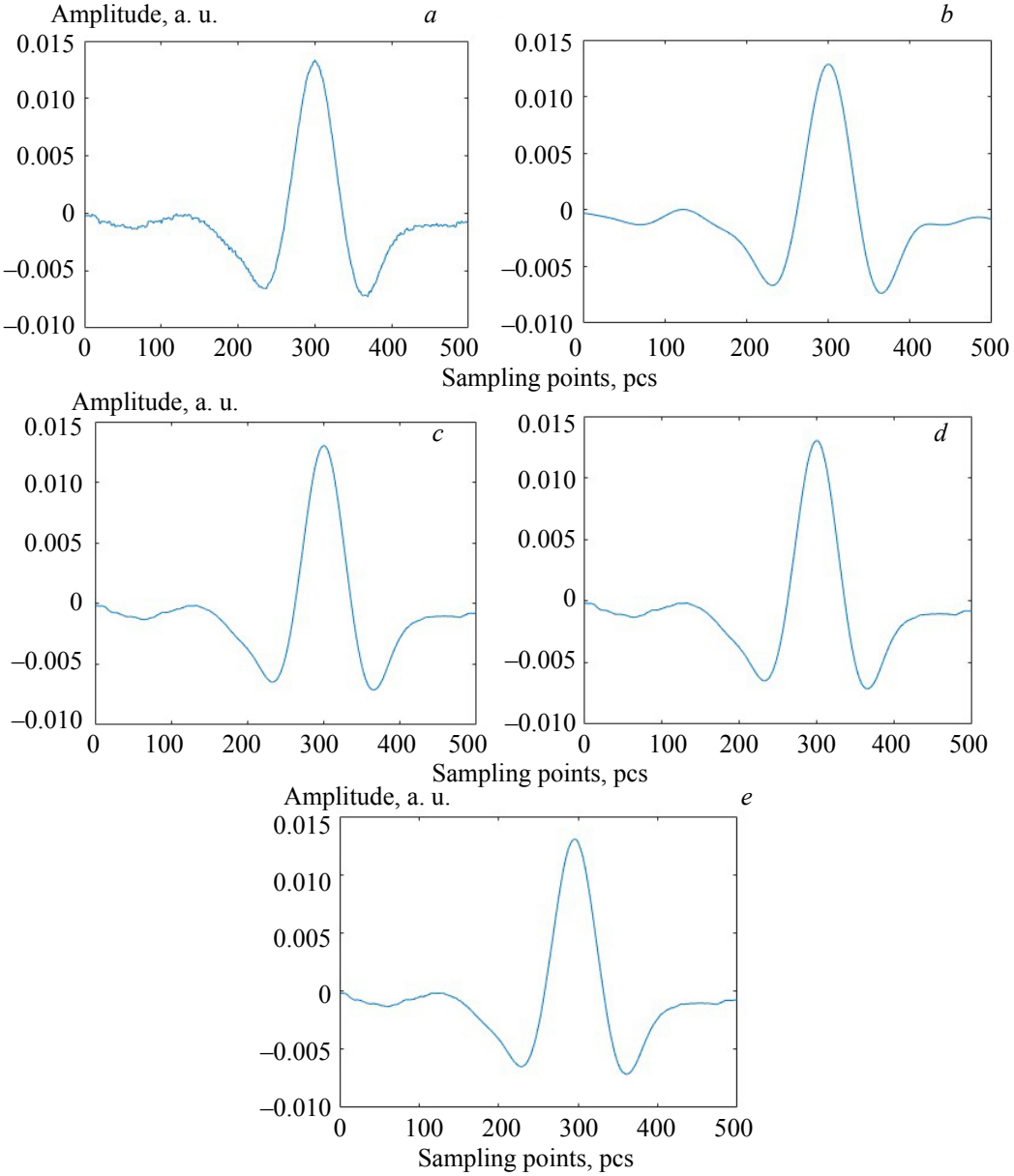

Fig. 7. Actual signal, SNR = 29.5 dB, R = 1.24 (a), SVD filtering, SNR = 86.5 dB, R = 0.78 (b), moving average filtering, SNR = 45.9 dB, R = 0.77 (c), wavelet filtering, SNR = 43.6 dB, R = 0.79 (d), and Kalman filtering, SNR = 47.3 dB, R = 0.77 (e).

It can be seen from the figures that the R values of the signal processed by the four algorithms are similar, but compared with the Kalman, moving average and wavelet transform algorithms, the SNR of the signal processed by the SVD algorithm is approximately twice as high as that of the other three methods. The experimental results indicated that the SVD method has the best filtering effect. The SNR is increased from 29.5 to 86.5 dB, and the noise removal rate is 66.7%; thus, these results can provide guidance for improving the TDLAS gas detection system to reduce noise.

Conclusions. To study the phenomenon of noise interference in TDLAS continuous harmonic detection technology, a simulation model of the TDLAS detection system and system noise is established. By comparing the four filtering algorithms, the best parameter settings for the four filtering algorithms to remove noise are analyzed and compared. It is concluded that the singular value decomposition method has the best filtering effect. The TDLAS detection system is designed, and the singular value decomposition method is used to process the second harmonic signal. The SNR after singular value processing increases from 29.5 to 86.5 dB, and the system noise removal rate is 66.7%. This method can reduce the system noise and effectively improve the detection accuracy, which is beneficial for subsequent data processing.

Acknowledgments. This research was financially supported by the Tianjin Municipal Education Commission (2017KJ057).

REFERENCES

1. G. Z. Gao, T. Zhang, G. Zhang, *Opt. Express*, **27**, No. 13, 17887–17904 (2019).
2. G. Zhang, G. Z. Gao, T. Zhang, X. Liu, C. D. Peng, T. D. Cai, *J. Quant. Spectrosc*., **241**, No. 34, 748 (2020).
3. J. Jiang, M. X. Zhao, G. M. Ma, *IEEE Sens. J*., **27**, No. 99, 1 (2018).
4. Y. Krishna, S. O'Byrne, K. Munuswamy, *Appl. Opt.*, **57**, No. 17, 4943 (2018).
5. J. D. Li, P. P. Zhang, Y. J. Ding, *Opt. Laser Eng*., **78**, No. 3-4, 503–511 (2020).
6. S. Pal, A. Das, S. Nandy, R. Kar, J. Ghosh, *Rev. Sci. Instrum*., **38**, No. 21, 4699 (2019).
7. K. Ruxton, A. L. Chakraborty, W. Johnstone, *Sensor Actuat. B*, **150**, No. 1, 367–375 (2010).
8. L. Li, N. Arsad, G. Stewart, *Opt. Commun*., **284**, No. 1, 312–316 (2011).
9. J. Reid, E. L. Sherbiny, B. K. Garside, *Appl. Opt. B*, **19**, No. 19, 3349–3353 (1980).
10. J. M. Poyet, Lutz Y. Light, *Opt. Eng*., **55**, No. 7, 75–103 (2016).
11. L. Persson, F. Andersson, M. Andersson, *Appl. Opt. B*, **87**, No. 3, 523–530 (2007).
12. S. Q. Wu, T. Kimishima, H. Kuze, *Appl. Phys*., **39**, No. 7A, 4034–4040 (2000).
13. P. W. Werle, P. Mazzinghi, F. D`Amato, *Spectrochim. Acta A*, **60**, No. 8-9, 1685–1705 (2004).
14. X. W. Zhou, H. F. Liu, *Laser Part Beams*., **20**, No. 8, 1262–1264 (2008).
15. J. S. Li, B. L. Yu, H. Fischer. *Appl. Spectrosc*., **69**, No. 4, 496–506 (2015).
16. D. B. Zou, W. L. Chen, Z. H. Du, *Spectrosc. Spectr. Anal*., **32**, No. 9, 2322–2326 (2012).
17. Y. L. Huang, Y. G. Zhang, X. D. Wang, *IEEE T. Instrum. Meas*., **60**(99), 1–14 (2017).
18. C. L. Li, Guo, X. Q. Guo, W. H. Ji, J. L. Wei, X. B. Qiu, W. G. Ma, *Opt. Quant. Electron*., **50**, No. 7, 1539 (2018).
19. D. S. Zhang, J. Guo, Y. Jin, *Opt. Eng*., **56**, No. 9, 1 (2017).